

# PLASMA ETCHING OF DEEP, HIGH-ASPECT RATIO FEATURES INTO FUSED SILICA

Dr. Michael Pedersen, *Member, IEEE* and Dr. Michael Huff, *Member, IEEE*

**Abstract**—This paper reports research performed on developing and optimizing a process recipe for the plasma etching of deep, high-aspect ratio features into fused silica (fused quartz) material using an Inductively-Coupled Plasma (ICP) Reactive-Ion Etch (RIE) process. As part of this effort, we performed a Design of Experiments (DOE) wherein the etch recipe parameters having the most impact on the etch process were varied over fixed ranges of predetermined values while the other etch recipe process parameters were unchanged. Subsequently, the etched samples were analyzed so as to quantify the etch outcomes. Using the experimental data collected during the DOE, we then performed multiple regression analysis on this data to determine optimal etch tool parameters in order to achieve the desired etch results. Based on this work, we have demonstrated the ability to etch very deep features into fused silica of over 100 microns, having nearly vertical sidewalls, and with aspect ratios of over 10 to 1 using the optimized etch process. The ability to fabricate deep, high-aspect ratio features into fused silica has important implications for a number of Micro-Electro-Mechanical Systems (MEMS) applications. The etch technology developments presented herein are applicable to fused silica as well as to other silicon-dioxide-based materials including crystalline quartz.

**Index Terms**— Inductively-coupled plasma (ICP) etching; Deep, high-aspect ratio plasma etching; fused silica; fused quartz; quartz; silicon dioxide; high Q materials; and Design of Experiments.

## I. INTRODUCTION

FUSED SILICA (fused quartz) has many very desirable material properties including: high quality (Q) factor, high stiffness, chemical inertness, high thermal stability, small visco-elastic losses, low thermal expansion, exceptionally good thermal shock resistance, low dielectric constant and low dielectric losses, good optical transparency ranging from deep ultraviolet to the far infrared, low thermal conductivity, and many others, making this material an excellent choice for many MEMS applications [1,2]. Additionally, quartz in a crystalline form is a piezoelectric material making it an excellent material choice for certain sensor, actuator, and electronic applications [3]. Likewise glass (e.g., silicon dioxide) also has many desirable properties for MEMS device applications [1,4]. These materials are important for use in

many MEMS device applications including resonators, gyroscopes, oscillators, microbalances, accelerometers, microfluidics, and others [5,6,7,8]. However, the fabrication technologies to shape and form these materials have been mostly limited to 19th century-based methods such as crystal cutting and wet etching techniques that lack accurate control of dimensions as well as other drawbacks.

Dry plasma etching of silicon dioxide has been around for a few years; however, this technology has been limited to depths of a few microns or less, very limited aspect ratios, and typically non-vertical sidewalls of the etched features [9,10]. Consequently, the ability to make very deep (more than 10's of microns), small-dimensional features with high aspect ratios and vertical etched sidewalls in these important materials has not been previously available to device developers.

We report in this paper the ability to etch very deep and high-aspect features into fused silica using a reactive ion etching process. We have demonstrated etches over 100 microns deep, with the capability of etching completely through 500 microns or thicker fused silica material layers or substrates. Moreover, this process can be used to make high-aspect ratio features (e.g., over 10 to 1) in fused silica and with nearly vertical sidewalls. As part of the work reported herein, we conducted a Design of Experiments (DOE) on the etch process in order to better understand this process, as well as how to optimize the process input parameters in order to obtain desired process outcomes such as highest etch rate and most vertical etched feature sidewalls.

## II. SILICON DIOXIDE PLASMA ETCHING

The mechanisms of plasma etching of silicon dioxide have been previously reported in the literature [11,12,13]. Zhang et al, provides an explanation of the mechanism which is summarized as follows: the etch process employs a continuous polymerization-dissolution process based on the ionization of  $C_xF_y$  fluorocarbons (including CF, CF<sub>2</sub>, C<sub>2</sub>F<sub>3</sub>, and C<sub>2</sub>F<sub>4</sub>); the polymers deposited onto the silicon dioxide surface partly dissolve the SiO<sub>2</sub> in a complicated interaction of fluorination, desorption and passivation. The dissolution of the fused silica occurs as a complex interaction between ions in the plasma and the solid fused silica resulting in the removal of glass and fluorocarbon polymer formation on the substrate. Due to the directionality of the incoming ions there is a preferential

removal direction of the polymer, which leads to anisotropy in the etched feature shape [11].

It has further been established that the addition of oxygen or argon to the plasma affects the polymerization rate in the process, since oxygen ions chemically attack the polymer and argon ions physically sputter the polymer [12]. Therefore, changes in etch rate, mask selectivity, and anisotropy (sidewall shape) can be realized with the introduction of these gases into the process chamber during etching.

This etch process has some significant differences compared to Deep, Reactive-Ion Etching (DRIE) of silicon using the Bosch<sup>TM</sup> process that is widely employed in MEMS fabrication technology. First, the SiO<sub>2</sub> etch is a continuous process and not switched or cycled between two process chemistries such as in the DRIE process. As a consequence, there is no scalloping of the sidewalls in SiO<sub>2</sub> as seen in silicon DRIE. Additionally, there is reduced lateral under-etching of the etch mask than is seen in silicon DRIE.

However, the etch rate of deep, high-aspect ratio SiO<sub>2</sub> etching is much slower compared to the DRIE of Si, and the SiO<sub>2</sub> etch process is more prone to micro-masking that can result in etch defects. Additionally, the mask selectivity is much lower in SiO<sub>2</sub> etching as compared to silicon DRIE and therefore a hard mask material may be used in SiO<sub>2</sub> etching.

Therefore, due to the unique attributes of SiO<sub>2</sub> plasma etching combined with the lack of research on deep etches into this material, as well as our need to develop an etch process recipe that result in high etch rate, high mask selectivity, and high aspect ratio, we conducted a Design of Experiments (DOE) to better understand this process and determine how to optimize the process parameters for desired outcomes.

### III. DESCRIPTION OF ETCH SYSTEM

The results of the etching experiments reported in this paper were performed on an ULVAC Technologies Neutral-Loop Discharge (NLD) 6000 etch system. This is a commercially available production-worthy Inductively-Coupled Plasma (ICP)-type of Reactive Ion Etch (RIE) tool that was specifically designed for the etching of hard to plasma etch materials including: fused silica (SiO<sub>2</sub>); silicon carbide (SiC); titanium dioxide (TiO<sub>2</sub>); tungsten silicide (WSi<sub>2</sub>); palladium (Pd); lithium niobate (LiNbO<sub>3</sub>); and others.

The basic diagram of the ULVAC NLD-6000 etcher system is shown in Figure 1. The tool uses a gas plasma wherein reactive ions impinge on the surface of the substrate to remove material from the substrate that is being etched through a combined chemical and mechanical effect. The system configuration employs an etch chamber connected to a vacuum pump to lower the pressure inside the chamber and transport process gases through the chamber. The substrate is positioned on a chuck that uses Helium backside cooling to control its temperature during etching.

Controlled amounts of chemically-reactive fluorocarbon process gases, such as Perfluoropropane (C<sub>3</sub>F<sub>8</sub>) Tetrafluoromethane (CF<sub>4</sub>), or Octafluorocyclobutane (C<sub>4</sub>F<sub>8</sub>), are introduced into the process chamber. Additionally, other gases such as Oxygen (O<sub>2</sub>) and/or Argon (Ar) may also be

introduced into the process chamber.

A plasma is generated by the interaction of the gases with a Radio Frequency (RF) electromagnetic field created by a coil operating at a frequency of 13.56 MHz connected to an RF generator. The RF coil encircles the etch chamber and is positioned outside the etch chamber. High-energy ions from the plasma are accelerated to strike the substrate surface by a separate Radio Frequency (RF) electromagnetic field created by a second RF generator operating at 13.56 MHz connected to the substrate chuck. In-line mass flow controllers control the flow rates of the process gases.

The ULVAC etcher employs three separate electromagnetic (EM) neutral coils positioned externally and encircling the etch chamber (See Figure 1). The current in these external EM coils are independently controlled thereby allowing the magnetic field shape and strength to be adjusted inside the chamber. This applied EM field directly impacts the plasma shape and density and has a pronounced effect on the spatial redistribution of the ions in the plasma inside the etch chamber. This capability enables the spatial redistribution of the ions in the plasma to enhance etching uniformity. This magnetic neutral loop discharge configuration can be used to simultaneously create a high-density plasma and low operating pressure (e.g., 10<sup>11</sup> cm<sup>-3</sup> at 10<sup>-1</sup> Pa) to enable high etch rates in hard to etch materials as well as enabling more anisotropic etching to be performed. Additionally, the bias voltage potentials on the antenna and substrate can also be independently controlled.

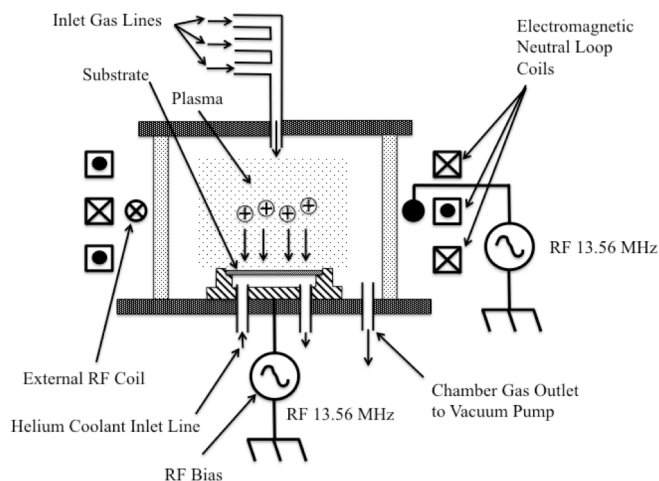


Figure 1: Basic cross-sectional diagram of ULVAC NLD etcher.

The ULVAC NLD-6000 etch system used in the present study is configured for use of CF<sub>4</sub>, C<sub>3</sub>F<sub>8</sub>, and C<sub>4</sub>F<sub>8</sub> fluorocarbon gases as well as oxygen (O<sub>2</sub>) gas. The tool can handle both 100-mm and 150-mm diameter substrates.

### IV. DESIGN OF EXPERIMENTS (DOE)

#### A. Outline of the Design of Experiments

All etching experiments in the present work were performed using perfluoropropane (C<sub>3</sub>F<sub>8</sub>) and oxygen (O<sub>2</sub>) as source gases on an ULVAC NLD-6000 etch system as described in Section III above.

The performance of a DOE on the etching process involves adjusting the independent process parameters that affect the etch process outcome in terms of depth and profile of the etched features in the material. A list of all the process parameters controlled by the etch system known to affect the etch outcome are shown in Table 1. As can be seen, we have identified a total of twelve (12) parameters that are known to affect the etch process for performing etches of fused silica. This essentially means that a DOE on this etch system would need to occur in a 12-dimensional space. However, performing a complete DOE on a 12-dimensional space is not practical since the number of experiments needed would be extremely large.

For the purposes of realizing a reasonably sized experimental space for the DOE while providing an acceptable trade-off between the amount of data required to optimize the process recipe versus the number of experiments, it was desirable to determine if it was possible to reduce the number of independent process parameters. We determined that four

TABLE I  
FUSED SILICA ETCH PROCESS PARAMETERS.

Chamber pressure	Substrate chuck temperature
C <sub>3</sub> F <sub>8</sub> flow	O <sub>2</sub> flow
RF Antenna power	RF Bias power
He cooling pressure	Upper magnet coil current
Center magnet coil current	Lower magnet coil current
Shield temperature	Chamber cleaning history

process parameters produce a much greater effect on the etch results than the others. The four selected parameters are highlighted in gray in Table 1 and include: chamber pressure; substrate chuck temperature; O<sub>2</sub> gas flow; and RF bias power.

Therefore, for each etch experiment performed in the DOE, one of the four most important process parameters was individually varied over three pre-determined process settings, while the remaining process parameters were unchanged. This was repeated for all four important process parameters. All process settings were based on a generic recipe from ULVAC.

The variations of the four selected process parameters were selected as percentage variations from the generic recipe as follows: RF bias power (0%; -33%; and 67%); chamber pressure (0%; -33%; and 67%); substrate temperature (0%; -25%; and 25%); and O<sub>2</sub>/C<sub>3</sub>F<sub>8</sub> gas mixture (0%; 17%; and 33%). These variations were based on our previous experience wherein we observed that these magnitudes of variations would provide sufficiently measureable differences in the etch outcomes even for only three separate settings.

It should be noted that the twelve (12) process parameters shown in Table 1 are not all of the experimental parameters that are known to affect the outcome of this etch process. Specifically, there are other experimental parameters that can also affect the etch outcome that are directly related to the substrates being etched. These other experimental parameters

include the material being etched, the mask material used, and the design configuration of the mask pattern used.

Because of the pronounced effect of feature size on the etch process, it was decided to record the actual feature size (mask opening) in each experiment and treat this data for DOE purposes as a fifth input parameter.

In the work presented herein, a total of sixty-four (64) different etch experiments were conducted and analyzed.

### B. Fabrication of Substrates Used in Design of Experiments

The substrates were made of fused silica, 100-mm in diameter with a nominal thickness of 500 microns. The etch times for each substrate during these experiments were based on the generic recipe that resulted in an etch depth of approximately 100 to 125 microns. However, as the process recipe was varied with the fixed etch times, the etch depths were observed to vary, as expected.

The fabrication process for the sample substrates used in the DOE is illustrated in Figure 2. An etch mask composed of electroplated nickel was fabricated on the surface of the substrates used in the study. The mask fabrication was performed by first depositing a thin plating base of gold onto the substrates (Figure 2 (a)), followed by the spin deposition of a photoresist layer that was nominally 20 microns in thickness. The photoresist was exposed and developed to clear regions on the substrate where the nickel would subsequently be electroplated (Figure 2 (b)). The substrate was then placed into an electroplating bath to plate approximately 20 microns of nickel in the open features in the photoresist (Figure 2 (c)). The photoresist was then removed using a solvent immersion (Figure 2 (d)). The thin layer of gold that acted as the plating base was removed using ion milling in the open areas where the polymer mold was located so as to expose the underlying surface of the fused silica (Figure 2 (e)).

For the nominal etch depths of 100-microns, we chose a 20-micron nickel mask thickness to ensure that the mask would remain after the etches were completed in the DOE. This decision was based on our past experience wherein the mask selectivity varied considerably depending on the process parameters.

Metrology on the substrates was performed prior to and after each etch (See Section V.). Additional metrology was performed on the substrates after removal of the mask including cross sectioning and inspection of the etched features using a scanning electron microscope (SEM).

As discussed above, a deposited polymer layer is an attribute of this process; this polymer layer was removed during the stripping of the mask using a series of aqua regia (1:3 ratio of nitric acid and hydrochloric acid) and piranha etches (3:1 ratio of sulfuric acid and hydrogen peroxide). Ultrasonic agitation was used to accelerate the cleaning process.

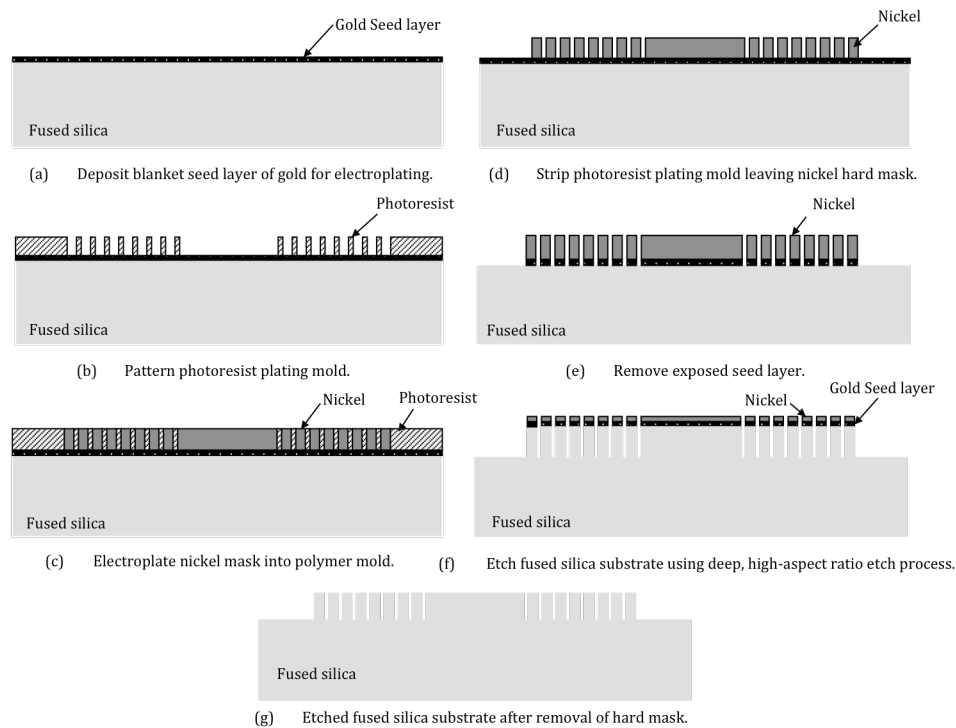


Figure 2: Illustration of the fabrication process sequence for the fused silica samples used in the design of experiments.

The mask layout on each fused silica sample substrate was designed so as to obtain a series of equally-spaced concentric circular rings of fused silica nominally having widths of 35 microns with approximately 25 micron gaps between the rings. This concentric ring pattern was stepped out uniformly over the 100-mm diameter fused silica substrates 10 times for a total of 10 etch test patterns across each substrate.

### V. METROLOGY COLLECTION PROCEDURE

The metrology data collection performed on the fused silica substrates etched during the DOE was based on the use of optical microscopy [Leica INS 1000 differential interference contrast optical microscope], scanning electron microscopy (SEM) [Hitachi S-4700 scanning electron microscope], and optical profilometry [WYKO model number NT-3300]. Using these methods of metrology a total of ten (10) characteristic etch result parameters labeled “A” through “S” as illustrated in Figure 3 and shown in Table 2 were derived for each substrate etched in the DOE. The procedure to process and collect the metrology data from the substrates etched during the DOE was as follows: a. perform pre-etch metrology inspection and collect data; b. etch the substrate using pre-selected DOE recipe; c. perform post-etch metrology inspection and collect data; d. clean substrate including removal of mask; and, e. perform cross-section metrology.

The metrology parameters illustrated in Figure 3 are for the fused silica substrate prior to the etch being performed (Figure 3 (a)), the fused silica substrate after the etch is performed but prior to removing the nickel hard mask and polymer (Figure 3 (b)), and the fused silica substrate after the etch and stripping of the nickel hard mask and polymer (Figure 3 (c)).

Each of these metrology parameters are tabulated in Table 2

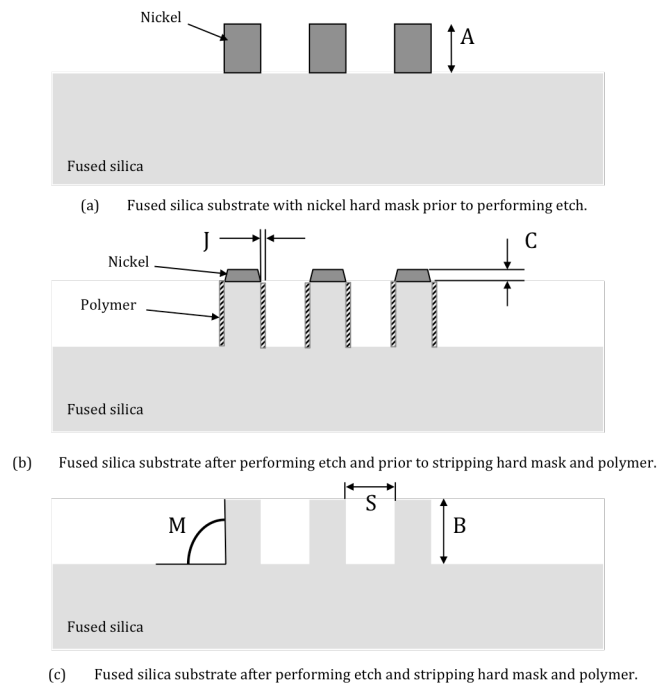


Figure 3: Illustration of the metrology

along with the name given to the parameters as well as how they were derived. Some of these parameters are directly measured (i.e., “A”, “B”, “C”, “J”, “M” and “S”) while others are calculated using the direct measurement data (i.e., “D”, “E”, “F”, “Q” and “R”).

The metrology performed was based on what would provide sufficient information to quantify the etch outcomes while also keeping the amount of data to reasonable levels. Metrology data was collected at designated locations on some or all of the test structures for each substrate. For single parameters, data

was collected at specific locations on selected die that were approximately in the middle of the substrate (e.g., die number 5). The etch uniformity “Q” was found by combining measurements from die number 5 and 8 near the middle and the periphery of each substrate, respectively. The etch quality “R” was evaluated by examination of die number 4.

Etch quality is defined by the lack of etch defects that were observed in the features etched into the fused silica. These etch defects were point defects that appeared to be caused by micromasking and bridging defects whereby some fused silica remained at a depth shallower than the etched bottom that extended across an etched feature. Figure 4 (a) shows a SEM image of an example of a bridging defect that extends from one of the fused silica rings into the etched trench and Figure 4 (b) shows an optical microscopy photograph of some point etch defects.

TABLE 2  
DOE WAFER METROLOGY PARAMETERS

Parameter	Parameter name	Derived from
A	Initial nickel mask thickness	Optical profilometry 10 points per wafer
B	Fused silica etch depth	Optical profilometry
C	Nickel mask thickness after etching	Optical profilometry & SEM
D	Fused silica etch rate	“B” divided by etch time
E	Mask selectivity	“B” divided by “F”
F	Nickel vertical etch rate	“A” minus “C” divided by etch time
J	Polymer thickness	SEM analysis
M	Top-to-bottom sidewall angle	SEM Cross-section analysis
Q	Etch depth uniformity	SEM Cross-section analysis Compare die #5 and #8
R	Etch quality	Microscope Inspection
S	Feature size to be etched	SEM

It should also be noted that some metrology measurements in Table 2, such as the polymer thickness, “J”, were extremely difficult to measure precisely, since the overall thickness of the layer was usually fairly small.

## VI. SUMMARY OF DATA COLLECTED IN DOE

A total of 154 individual metrology data points were collected per substrate resulting in a total of 9856 individual metrology data points for the entire DOE. A complete listing of all collected metrology data on the DOE wafers would be prohibitively lengthy. Therefore, an overview summary of the data collected during the DOE is presented in Table 3 showing six selected process output parameters relevant to fused silica etching. These six output parameters include: mask selectivity “E”; top-to-bottom sidewall angle “M”; polymer thickness “J”; fused silica etch rate “D”; etch depth uniformity “Q”; and etch quality “R.”

The definitions of these six output parameters and the desirable outcomes of these parameters are as follows: The mask selectivity (unit-less), “E,” is defined as the ratio of the etch rate of the fused silica to the etch rate of the nickel hard etch mask. A high mask selectivity is desirable since it allows a thinner mask to be used, and consequently, allows

greater dimensional control of the mask features and the etched features.

The top-to-bottom sidewall angle (degrees), “M,” is the angle of the sidewall with respect to a normal orthogonal from the substrate surface. A top-to-bottom sidewall angle of 90-degrees is more desirable since it represents the highest level of anisotropy of the etched features.

The polymer thickness (microns), “J,” is the thickness of the polymer material on the sidewalls of the etched features at the conclusion of the etch. A thinner layer of polymer is preferred since this lessens the difficulty of removing it. Additionally, if the polymer layer deposition becomes sufficiently thick, it

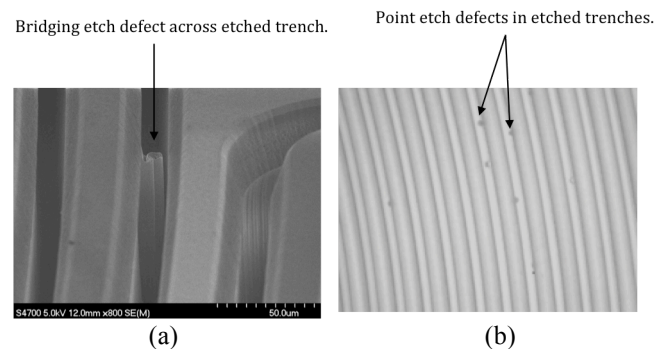


Figure 4: Test structure numbering scheme on each fused silica substrate etched during DOE.

can pinch off the etching process.

The fused silica etch rate (nanometers per second), “D,” is the rate at which the fused silica is removed. A higher etch rate is preferred since this allows the etching time to be

TABLE 3  
SUMMARY OF ETCH OUTCOME PARAMETERS FROM DATA COLLECTED DURING DOE.

Etch Outcome Parameter	Units	Range of Values in DOE Data
Mask Selectivity “E”	No units	8.2 to 17.3
Top-to-Bottom Sidewall Angle “M”	Degrees	76.6 to 90.2
Polymer Thickness “J”	Microns	2.0 to 9.8
Fused Silica Etch Rate “D”	Nanometers/sec	129.7 to 539.0
Etch Depth Uniformity “Q”	Percent (%)	0.1 to 39.4
Etch Quality “R”	No units	1 to 10

minimized, which in turn lowers the cost of the etch process.

The etch depth uniformity (%), “Q,” is the statistical uniformity of the etch depth across the etched features across the substrate. A higher level of etch depth uniformity is preferred since this allows better dimensional control and reduces the need for over-etching to clear all of the features.

Lastly, the etch quality (unit-less), “R,” is a score between 1 and 10 of the amount of defects observed in the etched features after the etch has been completed. A lower score representing a smaller number of etch defects is preferred.

The range of values in the six etch outcome parameters shown in Table 3 are sufficiently large to indicate that the three different values of input recipe settings selected in the DOE were of sufficient magnitude to provide discernable differences in the etch outcomes. Some of these ranges are remarkable. For example, the etch rate of fused silica,

parameter labeled “D,” had a low number of around 130 nm/sec while the high number was nearly 540 nm/sec, representing an increase of greater than 400% in etch rate from the low to high values. The etch depth uniformity, “Q,” had a low value of 0.1% that is at the limit of what can be measured, to a high value of over 39% indicative of a very non-uniform etch across a substrate.

It should also be noted that the DOE data does not show any obvious correlations in the process settings and outcomes. That is, none of the DOE experiments displayed optimums in all the six or even a majority of the outcome parameters. Therefore, more sophisticated analytical techniques are required in order to derive optimal recipes from the experimental results of the DOE

## VII. MULTIPLE REGRESSION ANALYSIS OF DATA COLLECTED IN DOE

For the analysis of the data collected during the DOE, a software package named DOE Pro XL from Sigmazone was utilized that is an extension to Microsoft Excel, allowing for use of all existing functionality within Excel and easy processing and sharing of the results.

The entire DOE data set was entered into the DOE Pro XL software package with the five selected independent input parameters, specifically: RF bias power; O<sub>2</sub>/C<sub>3</sub>F<sub>8</sub> gas mixture; substrate temperature; chamber pressure; and feature size. For the data analysis considered in this paper, five DOE output characteristics were selected as follows: mask selectivity, top-to-bottom sidewall angle, etch depth uniformity, etch quality, and etch rate. These five characteristics were deemed to be the most influential to achieve an optimized process for a deep, high-aspect ratio fused silica etch recipe. The software was then utilized to perform a multiple regression (y-hat) analysis with all of the one-way, two-way, parabolic, and three-way effects between the five independent input parameters. Importantly, only the effects having a high statistical significance in the model (specifically those having a P(2 tail) value of 0.05 or less) were included.

There are several statistical parameters of the regression model that were calculated based on our data and model. The “std error” value is a measure of the error of prediction of the model and this statistical parameter was found to be 1.9 for etch selectivity, 2.7 degrees for sidewall angle, 11% for etch uniformity, 2.2 for etch quality, and 32.2 nm/min for etch rate.

Additionally, there is the R-squared value, which is a measure of how well the model fits the actual recorded data. From our data, the R-squared value was found to vary between ~0.70 and ~0.98 across the five dimensions, thereby indicating a good fit between the model and the actual data. However, the adjusted R-square values that take into account the number of dependencies in the model and the number of actual experiments have values ranging from ~0.21 to ~0.93 and therefore are smaller and more spread out for the five dimensions. Additionally, the “F” and “Sig F” values, which are calculated from the regression coefficients in a statistical F-test, provide a measure of the model’s significance for

prediction. In order for a model to be considered significant for prediction, the “F” value should be larger than 6 and the “Sig F” value should be less than 0.05. The “F” values range from 1.5 to 23.6 and the “Sig F” values range from 0 to 0.2. This indicates some limitation of the model’s precision.

There are two possible options to improve the predictive quality of the model: acquire more experimental data, or reduce the number of effects considered. The consequence of reducing the number of effects is a model with better predictive quality, but a worse fit (R-squared) with actual data. Therefore, we performed a second multiple regression (y-hat) analysis with a total of 15-degrees of freedom that considered most of the relevant one-way, two-way, parabolic, and three-way effects between the five independent input parameters. In this second model, only the effects with P(2 tail) values of 0.2 or less were included in the model.

This second model resulted in “F” and “Sig F” values that satisfied the prediction ability criteria mentioned above (with the exception of “F” for the Etch selectivity and Etch quality), but the R-squared values have now declined to ~0.25 to ~0.95. While the simplified model is statistically more relevant, it does a less precise job of matching the actual data. Table 4 is the y-hat regression model for the DOE data collected using the reduced effects.

## VIII. DEMONSTRATION OF DOE RESULTS

Using the data from the DOE and the least squares data fitting capability of the Sigmazone Pro XL software, optimum processes within the DOE space that best meet specified criteria can be found. For each output variable considered it is possible to optimize to maximum, minimum, fixed value or value range criteria. In addition, each criterion is assigned a weight significance number (1=lowest to 100=highest). The weight significance number is selected and reflects the relative importance of the given criterion in finding a suitable solution. For the optimization of etching fused silica, it was decided to use the criteria and weights shown in Table 5. In the first optimization (A), some deterioration in etch quality might be allowed in the attempt to maximize the mask selectivity. In the second optimization (B), the etch quality must be at least as good as the baseline process.

Using the data from the DOE with these weighted goals, we derived an optimized process recipe for obtaining maximum etch rate and vertical sidewalls (90deg +/-0.5deg). The optimized process recipe to obtain these results is as follows:

RF Bias Power: 200 Watts  
 Substrate temperature: 15 °C  
 O<sub>2</sub> gas flow: 9 sccm  
 Chamber pressure: 5 mTorr  
 C<sub>3</sub>F<sub>8</sub> gas flow: 30 sccm  
 RF antenna power: 1950 Watts  
 Top magnet current: 6.1 Amps  
 Center magnet current: 10.2 Amps  
 Bottom magnet current: 6.1 Amps  
 Heat shield temperature: 150 °C  
 He cooling pressure: 5 Pascals

TABLE 4  
REDUCED EFFECTS Y-HAT REGRESSION MODEL FOR DOE DATA.

Y-hat Model		Selectivity				Wall angle				Uniformity				Etch quality				Etch rate			
Factor	Name	Coeff	P(2Tail)	Tol	Active	Coeff	P(2Tail)	Tol	Active	Coeff	P(2Tail)	Tol	Active	Coeff	P(2Tail)	Tol	Active	Coeff	P(2Tail)	Tol	Active
Const		12.037	0.0000			86.551	0.0000			0.95485	0.0000			3.952	0.0000			371.12	0.0000		
A	RF Power (W)									-0.06240	0.0017	0.8940	X					140.40	0.0000	0.7899	X
B	Temperature (degC)													0.59741	0.1118	0.8548	X				
C	O2 (sccm)					2.132	0.0000	0.9320	X	0.02466	0.3007	0.7207	X	0.25842	0.5034	0.8130	X	31.762	0.0000	0.9259	X
D	Pressure (mT)									-0.11297	0.0000	0.8962	X	-1.810	0.0000	0.9851	X	37.298	0.0000	0.8640	X
E	Initial gap (um)																	40.747	0.0003	0.7545	X
AA										0.10881	0.0439	0.9247	X					-43.598	0.0027	0.9209	X
AC		-1.414	0.0008	0.9369	X									-0.42060	0.3277	0.8008	X	-14.724	0.0188	0.9071	X
AD						2.316	0.0000	0.9763	X									18.939	0.0043	0.7883	X
BC		0.47284	0.2679	0.9758	X																
BE														-1.115	0.1515	0.8596	X				
CC														1.009	0.0889	0.9869	X				
CD						2.014	0.0002	0.9161	X	0.05148	0.0646	0.7860	X								
CE														-0.88658	0.3206	0.6943	X				
ACD		-0.91500	0.0616	0.9234	X					0.01697	0.5673	0.8159	X								
ACE										0.01622	0.7640	0.7697	X								
	R <sup>2</sup>	0.2526				0.5502				0.5295				0.4690				0.9515			
	Adj R <sup>2</sup>	0.2038				0.5209				0.4510				0.3805				0.9434			
	Std Error	1.9499				2.2539				0.1130				1.9530				29.4938			
	F	5.1813				18.7573				6.7514				5.2987				117.7271			
	Sig F	0.0036				0.0000				0.0000				0.0002				0.0000			
	F <sub>LOF</sub>	0.7622				1.3470				0.5578				1.6392				NA			
	Sig F <sub>LOF</sub>	0.7344				0.2335				0.8974				0.3421				NA			
	Source	SS	df	MS		SS	df	MS		SS	df	MS		SS	df	MS		SS	df	MS	
	Regression	59.1	3	19.7		285.9	3	95.3		0.6	7	0.1		141.5	7	20.2		71682.6	7	102408.9	
	Error	174.9	46	3.8		233.7	46	5.1		0.5	42	0.0		160.2	42	3.8		36535.1	42	869.9	
	Error <sub>NAE</sub>	106.6	25	4.3		130.6	29	4.5		0.2	10	0.0		9.7	4	2.4		NA	0	NA	
	Error <sub>LOF</sub>	68.3	21	3.3		103.1	17	6.1		0.3	32	0.0		150.5	38	4.0		NA	0	NA	
	Total	234.0	49			519.6	49			1.1	49			301.7	49			753397.8	49		

Additionally, the etch cycle time was 30 minutes, with an Oxygen (O2) clean cycle time of 30 seconds that is performed between each etch cycle. Using the above process parameter settings according to the model is predicted to result in an etch rate of 571 nm/min and etched feature sidewalls having an angle of 90deg +/-0.5deg.

We fabricated a test fused silica sample substrate using the fabrication process outlined in Figure 2 and performed an etch on this sample using the optimized process recipe recited above. The etch using this optimized process recipe was conducted for a total etch time of 200 minutes.

TABLE 5  
WEIGHTED GOALS USING REGRESSION MODEL FOR OPTIMIZATION  
(FEATURE SIZE SET TO 25UM).

<b>Optimization criteria</b>		
Criterion	Weight (0-100)	
	Process A	Process B
Maximize mask selectivity	70	70
Sidewall angle 90° ±0.5°	50	50
Etch depth uniformity <5%	30	30
Etch quality ≤3	50	100

A SEM image of the cross section of this sample substrate is shown in Figure 5. As can be seen, the recipe provided an etch that was deep and high in aspect ratio. The depth of the etched features was slightly over 100 microns, thereby resulting in an etch rate of about 500 nanometers/minute. Measurement of the sidewall angles indicated that they were 89.1 degrees or nearly vertical. The mask etch selectivity was measured to be approximately 10:1. The results of the etched

demonstration sample substrate are in close agreement with the predicted values from our model and therefore substantiate the validity of the model developed in the present work.

IX. CONCLUSIONS

We report on the development of a plasma etch process for implementing deep, high-aspect ratio features in fused silica. Specifically, we have demonstrated the ability to etch features into fused silica of more than 200 microns, having nearly vertical sidewalls, and aspect ratios of over 10 to 1 using an optimized process recipe developed in this work. We believe that this is the deepest etch ever reported in this type of material using a plasma etch process. To develop this optimized process recipe, we performed a design of experiments (DOE) in which a total of 64, 100-mm diameter nominally 500-micron thick fused silica substrates were etched. Extensive metrology was performed on each substrate before and after the etch, resulting in the collection of 9856 individual metrology data points. A multiple regression (y-hat) model of the data collected in the DOE was constructed and analyzed. This model included one-way, two-way, parabolic, three- and four-way interactions. Based on weighted values we selected on etch outcomes, we developed an optimized process recipe to obtain maximum etch rate and vertical sidewalls. We substantiated the predictive capability of our model by etching a fused silica substrate using the optimized process recipe, and the agreement between the model and the etch outcome was found to be very good with a measured etch rate of about 500 nm/min and sidewall angles of 89.1 degrees. Moreover, the resultant aspect ratio of the

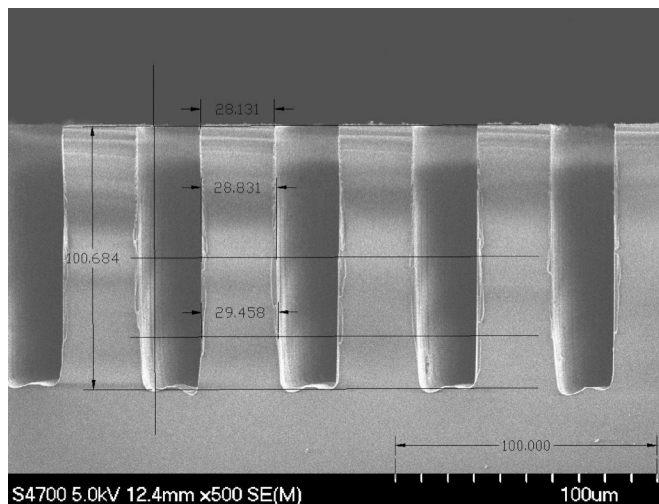


Figure 5: Scanning electron microscope (SEM) image of a cross section of fused silica sample after performing optimized process etch recipe for maximum etch rate and vertical or nearly vertical sidewall angle.

etched features were measured to be approximately 10 to 1. This process recipe may be used for etching fused silica to deeper etches than demonstrated herein, even for etching completely through substrates (i.e., for through-substrate via [TSV] processes). While the process recipe presented herein was developed on fused silica, it should be transferable to the etching of other silicon-dioxide-based materials including crystalline quartz. The ability to fabricate deep, high-aspect ratio features into fused silica is useful for several important MEMS applications such as high-performance inertial sensors, oscillators, and resonators. The etch process reported herein offers a new capability for the fabrication of MEMS devices and structures in hard to etch materials, such as fused silica and quartz, that employ large out-of-substrate-plane dimensions, high-aspect ratios, and large masses in comparison to previously available methods that either resulted in much shallower etch depths (using plasma etching methods) or loss of etch dimensional control (using wet etching techniques).

#### ACKNOWLEDGEMENT

This research was developed with funding from the Defense Advanced Research Projects Agency (DARPA). The views, opinions, and/or findings contained in this article are those of the authors and should not be interpreted as representing the official views or policies of the Department of Defense or the U.S. Government.

#### REFERENCES

- [1] De Jong, Bernard H. W. S.; Beerkens, Ruud G. C.; Van Nijnatten, Peter A. (2000). "Glass". Ullmann's Encyclopedia of Industrial Chemistry.
- [2] Penn, Steven D.; Harry, Gregory M.; Gretarsson, Andri M.; Kittelberger, Scott E.; Saulson, Peter R.; Schiller, John J.; Smith, Joshua R.; Swords, Sol O. (2001). "High quality factor measured in fused silica". *Review of Scientific Instruments* 72 (9): 3670.
- [3] Tanaka, M., "An overview of quartz MEMS devices," Frequency Control Symposium (FCS), IEEE International Conference, Newport Beach, CA, June 1-4, 2010.

- [4] Voskerician, G., et al., "Biocompatibility and biofouling of MEMS drug delivery devices," *Biomaterials*, Vol. 24, pp. 1959-1967. November 2003.
- [5] Johnson, R. Collins, "Quartz MEMS usher smallest real-time clock," *EETimes Asia*, December 12, 2008.
- [6] Stratton, F.P., et al., "A MEMS-based quartz resonator technology for GHz applications," *Frequency Control Symposium and Exposition, Proceedings of the IEEE International Conference*, August 23-27, 2004.
- [7] Jaruwongrunsee, K., et al., "Analysis of Quartz Crystal Microbalance Sensor Array with Circular Flow Chamber," *International Journal of Applied Biomedical Engineering*, Vol. 2, No. 2, 2009.
- [8] Liang, J., et al., "Realization of quartz MEMS accelerometer based on flip chip process," *IEEE 8th International Conference on Nano/Micro Engineered and Molecular Systems (NEMS)*, April 7-10, 2013.
- [9] Wang, S., et al., "Optimized condition for etching fused-silica phase gratings with inductively coupled plasma technology," *Applied Optics*, Vol. 44, No. 21, July 20, 2005, pp. 4429-4434.
- [10] Dauksher, W. J., et al., "Modeling and experimental data using a new high rate ICP tool for dry etching 200 mm EPL masks," *Microelectronic Engineering*, 61-62, 2002, pp. 887-894.
- [11] Zhang, D., and Kushner, M.J., "Reaction Mechanisms and SiO<sub>2</sub> Profile Evolution in Fluorocarbon Plasmas." Presentation given at 47<sup>th</sup> AVS International Symposium, October, 2000.
- [12] Sankaran, A., and Kushner, M. J., "Etching of porous and solid SiO<sub>2</sub> in Ar/c-C<sub>4</sub>F<sub>8</sub>, O<sub>2</sub>/c-C<sub>4</sub>F<sub>8</sub> and Ar/O<sub>2</sub>/C<sub>4</sub>F<sub>8</sub> plasmas," *Journal of Applied Physics*, vol. 97, 2005.
- [13] Fukasawa, T., et al., "Conelike Defect in Deep Quartz Etching Employing Neutral Loop Discharge," *Jpn. Journal of Appl. Phys.*, Vol 42, Part 1, No. 10, October 2003, pp. 6691-6697.



**Dr. Michael Pedersen** is an engineering professional in charge of special projects at the MNX. Dr. Pedersen has a Ph.D. degree in Electrical Engineering from the University of Twente, The Netherlands and a M.Sc. degree in Electrical Engineering from the Technical University of Denmark. He has more

than ten years of hands-on experience in MEMS technology from industrial and academic settings and is considered one of the world's foremost experts in acoustical MEMS devices. His most immediate industrial work assignment was at Knowles Electronics in Itasca, Illinois where he developed MEMS acoustical devices now being sold as microphones in the cell phone and hearing aid markets.



**Michael Huff** is Founder and Director of the MNX in Reston, Virginia, which was established to provide access to MEMS implementation resources, and develop manufacturing techniques. Dr. Huff has held a variety of notable positions working to advance and mature MEMS. Prior to establishing the MNX, Dr. Huff was on the faculty in the

Department of Electrical Engineering at Case Western Reserve University (CWRU) in Cleveland, Ohio. His research was focused on developing MEMS microfluidic components, including a novel MEMS-based insulin pump. Prior to joining CWRU, he was a Fellow of the Baxter Inc. where he managed product development efforts involving MEMS and other technologies. His primary research interests are in new microsystems fabrication techniques and microsystems manufacturing. Dr. Huff received a Ph.D. from MIT in Electrical Engineering and Computer Science (EECS).